Journal of Positive Sciences (JPS) eISSN: 2582-9351, https://positive-sciences.com JPS. 2026 Jun; 6(4): 69-92

Article info
Received on: 05.05.2026
Accepted on: 06.06.2026
Published on: 13.06.2026
doi: https://doi.org/10.52688/ASP74173

Research Article

Thermal Processing Effects on Mechanical Integrity and Fatigue Performance of CK45 Carbon Steel

Haitham Mohammed Ibrahim Al-Zuhairi [1], Iqbal alshalal [2], Hind H. Abbood [3], Mohammed RASHEED [4, *]

[1, 2, 3] Training and Workshop Center, University of Technology- Iraq, Baghdad, Iraq
[4] Production Engineering & Metallurgy College, University of Technology- Iraq, Baghdad 10066, Iraq

[*] rasheed.mohammed40@yahoo.com

ABSTRACT

CK45 medium-carbon steel is extensively employed in automotive, agricultural, and industrial applications owing to its favorable combination of strength, machinability, and cost-effectiveness. Nevertheless, components manufactured from CK45 steel are frequently exposed to cyclic loading environments where mechanical integrity and fatigue reliability are of paramount importance. In the present study, the influence of thermal processing on the microstructure, mechanical properties, and fatigue performance of CK45 carbon steel was systematically investigated using four representative conditions: as-received (S1), normalized (S2), quenched (S3), and quenched–tempered (S4). Optical microscopy, FESEM, and AFM analyses were performed to evaluate the microstructural evolution and surface characteristics, while Rockwell hardness, tensile, Charpy impact, and rotating bending fatigue tests were employed to assess the mechanical behavior. The results demonstrated that normalization refined the ferrite–pearlite structure and improved the overall performance, increasing the hardness from 18.6 ± 0.5 HRC to 22.8 ± 0.7 HRC, the yield strength from 425 ± 8 MPa to 485 ± 10 MPa, the ultimate tensile strength from 680 ± 12 MPa to 745 ± 15 MPa, and the fatigue limit from 290 ± 10 MPa to 340 ± 12 MPa. Quenching produced a predominantly martensitic microstructure, resulting in the highest hardness (55.4 ± 0.9 HRC), yield strength (1015 ± 18 MPa), and ultimate tensile strength (1185 ± 20 MPa), but significantly reduced the elongation (8.2 ± 0.4%) and impact toughness (18 ± 2 KJ) because of increased brittleness and residual stresses. Subsequent tempering transformed the brittle martensitic structure into tempered martensite with finely dispersed carbides, leading to a superior balance of properties, including a hardness of 44.1 ± 0.8 HRC, yield strength of 860 ± 15 MPa, ultimate tensile strength of 985 ± 18 MPa, elongation of 14.6 ± 0.5%, impact energy of 68 ± 3 KJ, fatigue limit of 395 ± 13 MPa, and fatigue life of 9.4×10^5 cycles at an applied stress of 500 MPa. Furthermore, AFM analysis revealed that the quenched specimen exhibited the highest surface roughness (R_a = 72.4 nm; R_{rms} = 91.8 nm), whereas the quenched–tempered condition showed the lowest roughness values (R_a = 28.9 nm; R_{rms} = 37.2 nm). The findings confirm that thermal processing is an effective strategy for tailoring the performance of CK45 steel. Among the investigated conditions, the quenched–tempered treatment emerged as the optimum route, providing the best compromise between strength, toughness, and fatigue reliability for engineering components operating under repeated loading conditions.

Keywords: CK45 carbon steel; thermal processing; heat treatment; mechanical integrity; fatigue performance

INTRODUCTION

CK45 is a medium-carbon steel containing approximately 0.42–0.50 wt.% carbon and is extensively utilized in the manufacturing of shafts, gears, bolts, crankshafts, couplings, connecting rods, and numerous machine components because of its favorable balance between strength, machinability, and economic cost [1]. Owing to its wide industrial application, CK45 steel is frequently exposed to dynamic service conditions involving

*Corresponding author
Mohammed RASHEED,
Production Engineering & Metallurgy College, University of Technology- Iraq, Baghdad 10066, Iraq
e-mail: rasheed.mohammed40@yahoo.com

repeated mechanical loading, impact forces, and fluctuating stresses. Under such conditions, both mechanical integrity and fatigue resistance become critical factors governing the reliability and service life of structural components [2]. Heat treatment is recognized as one of the most effective methods for tailoring the microstructure of carbon steels and improving their performance characteristics. By controlling heating and cooling schedules, thermal processing can significantly alter phase composition, grain size, residual stress distribution, and dislocation density, thereby modifying the overall behavior of the material [3]. Thermal processing techniques including normalizing, quenching, and tempering have profound effects on the microstructural evolution of CK45 steel. Normalizing refines the ferrite–pearlite structure and enhances the uniformity of grain distribution, resulting in improved strength and toughness. Quenching promotes the transformation of austenite into martensite, producing substantial increases in hardness and tensile strength. However, the high internal stresses associated with martensitic structures often reduce ductility and impact resistance. Tempering following quenching alleviates residual stresses and transforms brittle martensite into tempered martensite, thereby restoring toughness while maintaining relatively high strength. Since fatigue crack initiation and propagation are strongly influenced by microstructure and residual stress states, the selection of appropriate thermal processing conditions plays a decisive role in determining fatigue life and structural reliability [4].

Although CK45 carbon steel is widely employed in engineering applications, premature failures due to fatigue remain a major concern, particularly in components operating under cyclic loading conditions [5]. Industrial heat treatment procedures are often selected based primarily on hardness or tensile strength requirements without comprehensive consideration of fatigue performance. Consequently, identifying a thermal processing route capable of simultaneously enhancing strength, toughness, and fatigue resistance remains a significant challenge. Previous investigations on CK45 steel have predominantly focused on evaluating either static mechanical properties or fatigue characteristics independently. Limited studies have systematically correlated the influence of different thermal processing conditions with both mechanical integrity and fatigue behavior using a unified experimental approach. Furthermore, comparative assessments involving as-received, normalized, quenched, and quenched–tempered conditions under identical testing procedures are scarce. This lack of integrated understanding motivates the present work to establish clear relationships between heat treatment, microstructural evolution, and fatigue performance [6].

The primary objective of this study is to investigate the influence of thermal processing on the mechanical integrity and fatigue performance of CK45 carbon steel. The work aims to provide a comprehensive understanding of how different heat treatment conditions modify the microstructure and consequently affect the material's mechanical behavior and fatigue resistance. To achieve this objective, the microstructural evolution associated with various thermal processing routes is systematically evaluated and correlated with changes in hardness, tensile properties, and impact toughness. In addition, the fatigue life and endurance characteristics of CK45 steel under cyclic loading conditions are assessed to determine the effect of thermal treatments on long-term structural reliability. By integrating microstructural characterization with mechanical and fatigue analyses, this study seeks to establish clear relationships between processing conditions and performance outcomes. Furthermore, the investigation aims to identify the thermal processing condition that offers the most favorable balance between strength, toughness, and fatigue resistance for practical engineering applications. The scope of this research is limited to four representative conditions of CK45 carbon steel, namely the as-received condition (S1), normalized condition (S2), quenched condition (S3), and quenched–tempered condition (S4), which are selected to represent the most commonly employed thermal treatments in industrial practice. The novelty of this study lies in providing a comprehensive and integrated evaluation of thermal processing effects on both the mechanical integrity and fatigue performance of CK45 carbon steel. Unlike previous studies that examined isolated properties, the present work combines microstructural characterization, hardness measurements, tensile testing, impact analysis, and fatigue evaluation to establish direct correlations between processing conditions and performance. The study further identifies the most suitable heat treatment condition for engineering applications subjected to repeated loading, thereby offering practical guidelines for material selection and component design. Several limitations should be acknowledged in this investigation. First, the experiments are conducted under laboratory conditions that may not fully represent actual service environments. Second, fatigue testing is limited to rotating bending conditions and does not include axial, torsional, or multiaxial fatigue loading. Third, environmental effects such as corrosion fatigue, elevated-temperature fatigue, and

*Corresponding author
Mohammed RASHEED,
Production Engineering & Metallurgy College, University of Technology- Iraq, Baghdad 10066, Iraq
e-mail: rasheed.mohammed40@yahoo.com

wear-assisted fatigue are beyond the scope of the present work. Finally, only four thermal processing conditions are considered, and other treatment parameters may also influence the observed behavior.
The remainder of this paper is organized as follows. Section 2 describes the materials used, specimen preparation procedures, thermal processing routes, and experimental methods employed for microstructural and mechanical characterization. Section 3 presents the results and discussion concerning microstructural evolution, hardness behavior, tensile properties, impact toughness, and fatigue performance under different thermal conditions. Finally, Section 4 summarizes the major findings of the study, highlights the engineering implications of the results, and provides recommendations for future investigations.

MATERIALS AND METHODS

MATERIAL SELECTION AND CHEMICAL COMPOSITION

Commercial CK45 medium-carbon steel was selected as the base material for this investigation because of its extensive use in engineering applications that require a combination of strength, toughness, and fatigue resistance. CK45 steel is commonly employed in the production of shafts, gears, pins, connecting rods, bolts, and various machine elements subjected to repeated loading conditions. The nominal chemical composition of CK45 steel generally conforms to international standards and consists of approximately 0.42–0.50 wt.% carbon, 0.50–0.80 wt.% manganese, ≤0.40 wt.% silicon, ≤0.045 wt.% phosphorus, ≤0.045 wt.% sulfur, with the balance being iron. Prior to specimen preparation, the chemical composition of the material was verified using Optical Emission Spectroscopy (OES) to ensure consistency with the specified CK45 grade.

SPECIMEN PREPARATION

The CK45 steel bars were machined into specimens suitable for different characterization techniques and mechanical tests. Standard machining procedures were employed to minimize the introduction of excessive residual stresses and surface defects that could influence fatigue behavior. Separate specimens were prepared for metallographic examination, hardness measurements, tensile testing, impact testing, and fatigue evaluation. The dimensions of the tensile specimens were prepared according to ASTM E8/E8M, whereas the impact specimens followed the ASTM E23 standard. Fatigue specimens were fabricated in accordance with ASTM E466 requirements for rotating bending fatigue tests. All specimen surfaces were carefully polished and finished to reduce surface irregularities that might act as crack initiation sites during cyclic loading.

THERMAL PROCESSING PROCEDURES

To investigate the influence of thermal processing on the mechanical integrity and fatigue performance of CK45 steel, four representative conditions were selected and designated as S1, S2, S3, and S4. The heat treatment schedules were designed to represent the most commonly used industrial thermal processing routes.

S1: As-Received Condition

The first group of specimens was retained in the as-received condition without any additional thermal treatment. These specimens served as the reference material against which the effects of subsequent heat treatments were evaluated. The microstructure of this condition was expected to consist predominantly of ferrite and pearlite formed during the original manufacturing process.

S2: Normalized Condition

For the normalized condition, the specimens were heated to 850 °C and maintained at this temperature for 60 minutes to ensure complete austenitization. Subsequently, the specimens were removed from the furnace and allowed to cool naturally in still air to room temperature. The normalizing process was intended to

*Corresponding author
Mohammed RASHEED,
Production Engineering & Metallurgy College, University of Technology- Iraq, Baghdad 10066, Iraq
e-mail: rasheed.mohammed40@yahoo.com

refine the grain structure, homogenize the microstructure, and improve the balance between strength and toughness through the formation of fine ferrite–pearlite colonies.

S3: Quenched Condition

The quenching treatment involved heating the specimens to 850 °C for 60 minutes followed by rapid cooling in oil. The rapid cooling suppressed diffusional transformations and promoted the formation of martensite. This microstructure is characterized by high hardness and strength; however, it may also introduce considerable residual stresses and brittleness. The quenched condition was selected to evaluate the maximum strengthening effect achievable through thermal processing.

S4: Quenched–Tempered Condition

Specimens assigned to the quenched–tempered condition were initially subjected to the same quenching treatment described for S3. Following quenching, the specimens were reheated to a tempering temperature of 400 °C and held for 60 minutes before being cooled in air. Tempering was performed to relieve residual stresses, reduce brittleness, and improve toughness while maintaining relatively high strength levels. The resulting tempered martensitic structure was expected to provide an optimum balance of mechanical and fatigue properties. The thermal processing conditions employed in this investigation are summarized in Table 1.

Table 1. Description of CK45 steel specimens and thermal processing conditions.

Sample Code	Specimen Description	Thermal Processing Route
S1	As-received CK45 steel	The specimens were used in the original condition without any additional heat treatment and served as the reference material.
S2	Normalized CK45 steel	The specimens were heated to 850 °C for 60 min to achieve complete austenitization and subsequently cooled in still air to room temperature.
S3	Quenched CK45 steel	The specimens were austenitized at 850 °C for 60 min followed by rapid cooling in oil to produce a martensitic structure.
S4	Quenched–tempered CK45 steel	After quenching at 850 °C for 60 min and oil cooling, the specimens were tempered at 400 °C for 60 min and then air cooled to improve toughness and reduce residual stresses.

METALLOGRAPHIC EXAMINATION

Microstructural characterization was carried out to investigate the phase transformations induced by the various thermal processing routes. The specimens were sectioned, mounted in epoxy resin, and prepared using a MetaServ 250 metallographic grinding and polishing machine (Buehler Ltd., USA) operating at variable rotational speeds ranging from 50 to 500 rpm. Sequential grinding was performed using silicon carbide abrasive papers of different grit sizes, followed by final polishing using diamond suspensions to obtain mirror-like surfaces. The polished specimens were etched with a 2% nital solution to reveal the microstructural features. Optical observations were conducted using an Olympus BX53M metallurgical microscope (Olympus Corporation, Japan) with a magnification range of 50×–1000×. Representative micrographs were captured to evaluate grain morphology, phase distribution, and microstructural refinement resulting from the applied thermal treatments.

FESEM ANALYSIS

The surface morphology and microstructural characteristics of the thermally processed CK45 steel specimens were further examined using Field Emission Scanning Electron Microscopy (FESEM). The observations were carried out using a JSM-7610F field emission scanning electron microscope (JEOL Ltd.,

*Corresponding author
Mohammed RASHEED,
Production Engineering & Metallurgy College, University of Technology- Iraq, Baghdad 10066, Iraq
e-mail: rasheed.mohammed40@yahoo.com

Tokyo, Japan). The instrument is equipped with a high-brightness Schottky field emission electron source and provides a magnification range from 25× to 1,000,000×, with a spatial resolution of 1.0 nm at 15 kV and 1.5 nm at 1 kV. Prior to examination, the specimens were ultrasonically cleaned in ethanol and dried under ambient conditions. The FESEM analysis was performed under high-vacuum mode using an accelerating voltage in the range of 5–20 kV to reveal the morphological features associated with the different thermal processing routes. The acquired micrographs were employed to investigate the evolution of ferrite–pearlite structures, the formation of acicular martensite after quenching, and the development of tempered martensite following tempering. The FESEM observations were subsequently correlated with the mechanical and fatigue properties to elucidate the influence of microstructural changes on the performance of CK45 steel.

ATOMIC FORCE MICROSCOPY (AFM)

The surface topography and roughness characteristics of CK45 steel specimens subjected to different thermal treatments were analyzed using Atomic Force Microscopy (AFM). The measurements were performed using an SPM-9700 atomic force microscope (Shimadzu Corporation, Kyoto, Japan) operating in tapping mode to minimize surface damage during scanning. The instrument offers a vertical resolution of approximately 0.01 nm, a lateral resolution of 0.2–1 nm, and a maximum scan range of 90 µm × 90 µm in the XY direction with a Z-range of 10 µm. For each specimen, several regions were scanned over an area of 10 µm × 10 µm at room temperature to ensure the reproducibility of the measurements. Both two-dimensional (2D) and three-dimensional (3D) topographic images were recorded, and the surface roughness parameters, including the average roughness (Ra) and root mean square roughness (Rrms), were calculated using the microscope software. AFM characterization was utilized to assess the effect of thermal processing on surface morphology and to establish correlations between surface roughness, microstructural evolution, and the mechanical and fatigue performance of CK45 carbon steel.

HARDNESS MEASUREMENTS

The hardness of the CK45 specimens was determined using a Wilson 574 Series Rockwell hardness tester (Wilson Hardness, Buehler, USA) in accordance with ASTM E18. The instrument operates using Rockwell hardness scales with test loads ranging from 60 to 150 kgf, and the hardness values were recorded on the HRC scale. At least five indentations were made at different locations on each specimen to minimize local variations and improve measurement reliability. The average hardness value and standard deviation were subsequently calculated and reported. The hardness results were used to assess the strengthening effect associated with the microstructures generated through different thermal processing conditions. Fig. 1 presents a schematic illustration of the Rockwell hardness testing procedure performed according to the ASTM E18 standard. The figure demonstrates the sequential stages involved in determining the Rockwell hardness value, beginning with the application of the minor load to establish a reference position, followed by the application of the major load to produce the indentation. Subsequently, the major load is removed while maintaining the minor load, and the residual indentation depth is measured and automatically converted into the corresponding Rockwell hardness number (HR). The diagram also highlights the geometry of the diamond cone (Brale) indenter used in the HRC scale, the loading conditions, and the typical testing parameters recommended by ASTM E18. This schematic provides a clear understanding of the operating principle of the Rockwell hardness test employed to evaluate the resistance of thermally processed CK45 steel specimens to localized plastic deformation.

*Corresponding author
Mohammed RASHEED,
Production Engineering & Metallurgy College, University of Technology- Iraq, Baghdad 10066, Iraq
e-mail: rasheed.mohammed40@yahoo.com

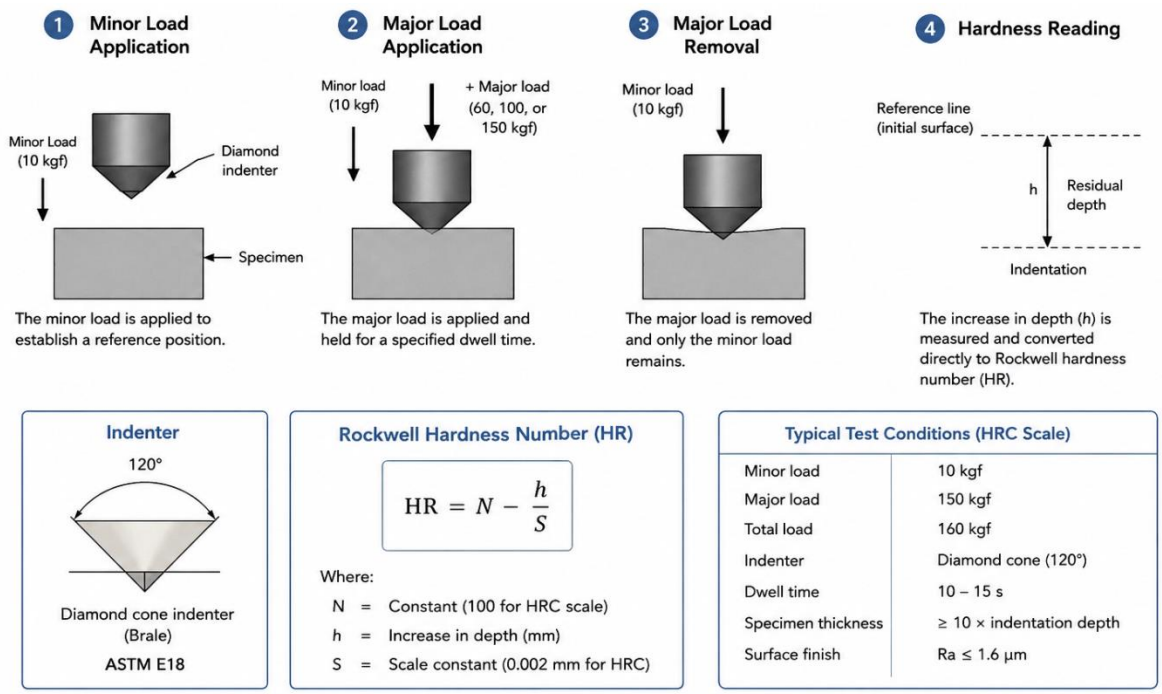

Fig. 1. Schematic illustration of the Rockwell hardness testing procedure according to ASTM E18, showing the sequence of minor load application, major load application, major load removal, hardness measurement principle, diamond cone (Brale) indenter geometry, and typical HRC testing conditions.

TENSILE TESTING

The tensile properties of CK45 steel were evaluated according to ASTM E8/E8M using an Instron 5982 Universal Testing Machine (Instron Corporation, USA) equipped with a maximum load capacity of 100 kN. Standard dog-bone tensile specimens were tested under monotonic loading at room temperature until fracture. The strain measurements were recorded using an Instron 2630-112 clip-on extensometer (Instron Corporation, USA) with a gauge length range of 12.5–50 mm and a strain capacity of ±10%. The obtained stress–strain curves were used to determine the yield strength, ultimate tensile strength, elongation at fracture, and elastic modulus of the investigated specimens. Fig. 2 presents a schematic representation of the tensile testing procedure conducted in accordance with the ASTM E8/E8M standard for evaluating the mechanical behavior of CK45 carbon steel specimens subjected to different thermal processing conditions. The figure illustrates the standard dog-bone tensile specimen geometry mounted between the upper and lower grips of the universal testing machine. During the test, a uniaxial tensile load is continuously applied at a controlled crosshead speed until specimen fracture occurs. The resulting load and elongation data are used to generate the engineering stress–strain curve, from which important tensile parameters, including yield strength, ultimate tensile strength, elongation at fracture, and elastic modulus, are determined. The schematic also highlights the gauge section of the specimen, where uniform deformation and strain measurements are recorded using an extensometer. Tensile testing provides essential information regarding the load-bearing capacity and ductility of thermally processed CK45 steel, thereby enabling direct comparison of the mechanical integrity associated with the as-received, normalized, quenched, and quenched–tempered conditions.

*Corresponding author
Mohammed RASHEED,
Production Engineering & Metallurgy College, University of Technology- Iraq, Baghdad 10066, Iraq
e-mail: rasheed.mohammed40@yahoo.com

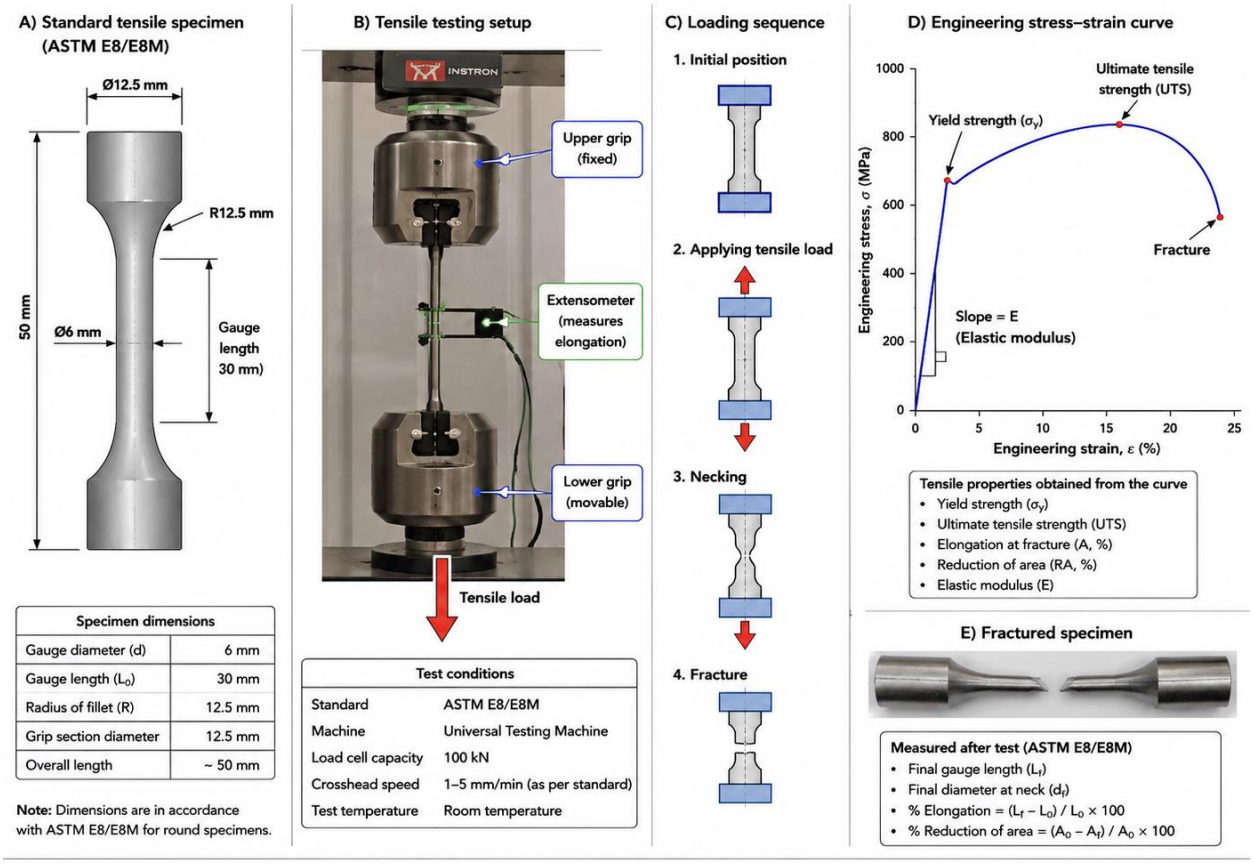

Fig. 2. Schematic illustration of the ASTM E8/E8M tensile testing setup showing the standard dog-bone specimen geometry, gripping arrangement in the universal testing machine, extensometer attachment at the gauge section, application of uniaxial tensile loading, and the corresponding engineering stress–strain curve used to determine yield strength, ultimate tensile strength, elongation, and elastic modulus of CK45 carbon steel specimens.

IMPACT TOUGHNESS EVALUATION

The impact toughness of the thermally processed CK45 steel specimens was evaluated using a JBW-300B Charpy impact testing machine (Time Group Inc., China) in accordance with the requirements of ASTM E23. The instrument has an energy capacity ranging from 0 to 300 J and is designed to determine the energy absorbed by metallic materials during sudden loading conditions. Standard V-notch specimens were prepared and tested at room temperature. During the experiment, the pendulum hammer was released from a predefined height to strike the notched specimen, and the energy absorbed during fracture was automatically recorded by the testing machine. The measured impact energy values were used to assess the ability of the various thermally processed specimens to resist crack initiation and propagation under dynamic loading conditions. The impact toughness results also provided valuable insight into the effectiveness of different heat treatments in improving the balance between strength and ductility of CK45 steel. Fig. 3 presents a schematic illustration of the Charpy V-notch impact testing procedure according to ASTM E23. The figure depicts the standard V-notch specimen geometry, specimen support arrangement, pendulum hammer trajectory before and after impact, and the determination of the absorbed impact energy from the difference between the initial and final pendulum heights. The schematic also highlights the principal dimensions of the V-notch specimen and the operating principle of the impact testing machine used to evaluate the toughness behavior of CK45 steel specimens subjected to different thermal processing conditions.

*Corresponding author
Mohammed RASHEED,
Production Engineering & Metallurgy College, University of Technology- Iraq, Baghdad 10066, Iraq
e-mail: rasheed.mohammed40@yahoo.com

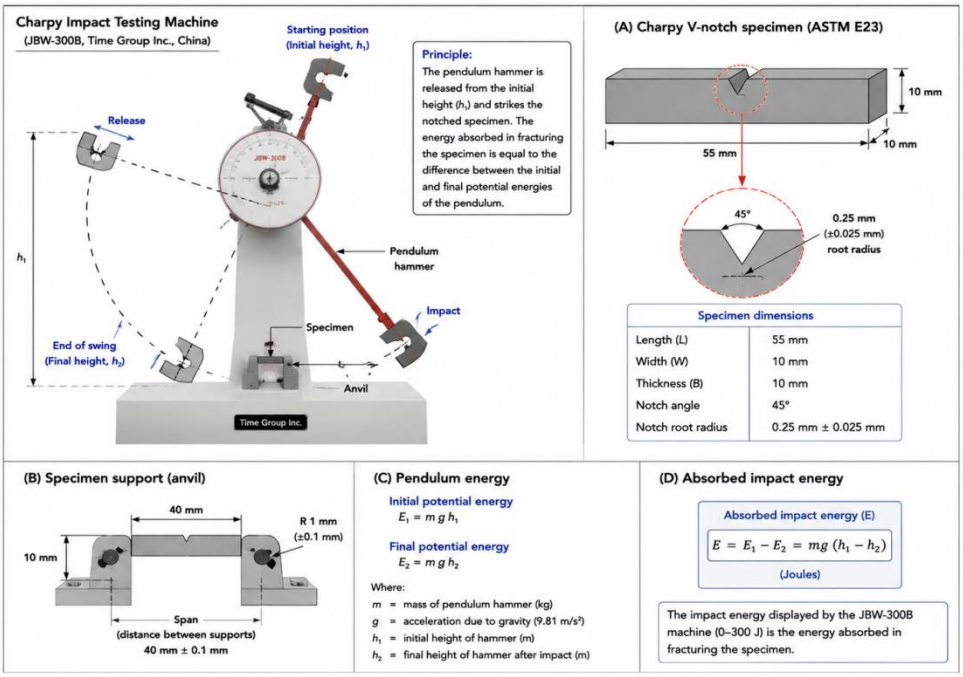

Fig. 3. Schematic illustration of the Charpy V-notch impact test according to ASTM E23, showing the standard specimen geometry, pendulum hammer motion, specimen support configuration, and determination of absorbed impact energy used to evaluate the impact toughness of thermally processed CK45 carbon steel specimens.

FATIGUE TESTING

Fatigue performance was investigated using a Tinius Olsen HSM19 rotating bending fatigue testing machine (Tinius Olsen, USA) in accordance with ASTM E466. The machine operates with a loading frequency between 50 and 100 Hz and can generate bending moments of up to 200 N·m. The fatigue specimens were subjected to completely reversed cyclic loading until failure or until reaching the predetermined run-out limit. The number of cycles to failure corresponding to each applied stress level was recorded, and the resulting data were used to construct S–N curves and determine the fatigue behavior and endurance characteristics of the different thermal processing conditions. Fig. 4 presents a schematic representation of the rotating bending fatigue testing procedure performed in accordance with ASTM E466 using a Tinius Olsen HSM19 fatigue testing machine. The figure illustrates the principal components of the fatigue testing system, including the machine configuration, standard fatigue specimen geometry, loading arrangement, and stress conditions developed during specimen rotation. The rotating bending mechanism generates completely reversed cyclic stresses (stress ratio, $R = -1$) on the specimen surface, thereby simulating the alternating loading conditions commonly encountered by engineering components during service. The figure further demonstrates the distribution of bending stresses along the specimen, the determination of the maximum bending stress, and the construction of the characteristic S–N curve, which relates the applied stress amplitude to the number of cycles to failure. The S–N diagram provides essential information regarding fatigue strength, endurance behavior, and the fatigue limit of the investigated material. Through this testing approach, the influence of thermal processing on the fatigue resistance and service reliability of CK45 carbon steel can be systematically evaluated and compared among the as-received, normalized, quenched, and quenched–tempered conditions.

*Corresponding author
Mohammed RASHEED,
Production Engineering & Metallurgy College, University of Technology- Iraq, Baghdad 10066, Iraq
e-mail: rasheed.mohammed40@yahoo.com

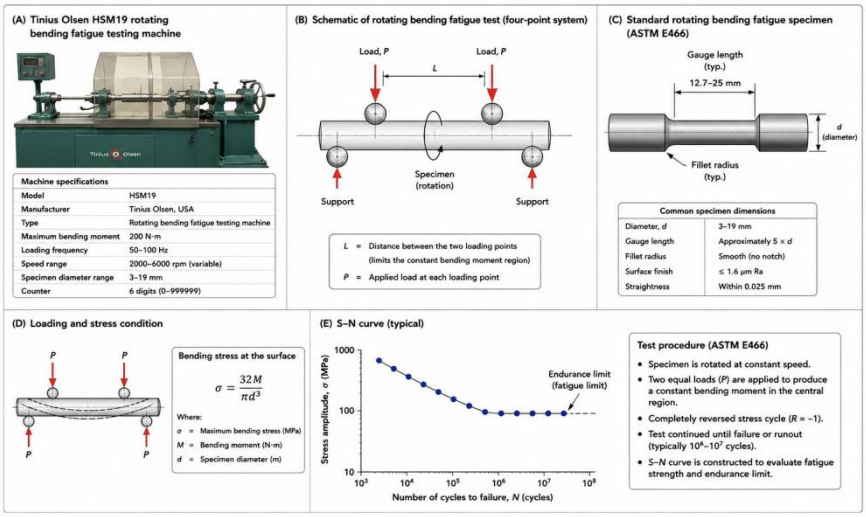

Fig. 4. Schematic illustration of the rotating bending fatigue test according to ASTM E466 using the Tinius Olsen HSM19 machine, showing (a) the fatigue testing apparatus and machine specifications, (b) the rotating bending loading configuration, (c) the standard fatigue specimen geometry, (d) the cyclic bending stress condition during specimen rotation, and (e) the typical S–N curve used to determine fatigue strength and endurance characteristics of thermally processed CK45 carbon steel specimens

FRACTOGRAPHIC ANALYSIS

Following fatigue testing, the fracture surfaces of selected specimens were examined using a JSM-IT200 Scanning Electron Microscope (JEOL Ltd., Japan) in accordance with ASTM E1508. The SEM provides a magnification range extending from 5× to 300,000×, enabling detailed examination of fatigue crack initiation sites, crack propagation regions, and final overload fracture zones. Prior to SEM observation, the fractured specimens were coated with a thin conductive layer using a Q150R ES sputter coater (Quorum Technologies, United Kingdom) capable of depositing metallic coatings with thicknesses ranging from 1 to 100 nm. The fractographic observations were correlated with the mechanical and fatigue results to clarify the influence of thermal processing on the failure mechanisms of CK45 steel. Fig. 5 presents representative fractographic features observed on the fatigue fracture surfaces of thermally processed CK45 steel specimens using scanning electron microscopy (SEM). The micrographs illustrate the typical stages of fatigue failure, including crack initiation, stable crack propagation, and final overload fracture. Fatigue cracks were generally initiated at surface imperfections, stress concentration regions, or microstructural discontinuities where cyclic stresses reached critical levels. The crack propagation region exhibited characteristic fatigue striations and progressive advancement of the crack front under repeated loading conditions. In the final stage of failure, rapid fracture occurred when the remaining cross-sectional area became insufficient to sustain the applied load, resulting in a distinct overload zone characterized by ductile dimples or cleavage features depending on the thermal condition of the specimen. Comparative fractographic analysis enabled the identification of the dominant failure mechanisms associated with the different heat treatment conditions. The quenched specimens typically showed relatively brittle fracture characteristics with cleavage-like features, whereas the quenched–tempered specimens exhibited more ductile behavior accompanied by fine dimples and improved resistance to crack propagation. These observations provided valuable insight into the relationship between microstructural evolution and fatigue performance of CK45 carbon steel.

*Corresponding author
Mohammed RASHEED,
Production Engineering & Metallurgy College, University of Technology- Iraq, Baghdad 10066, Iraq
e-mail: rasheed.mohammed40@yahoo.com

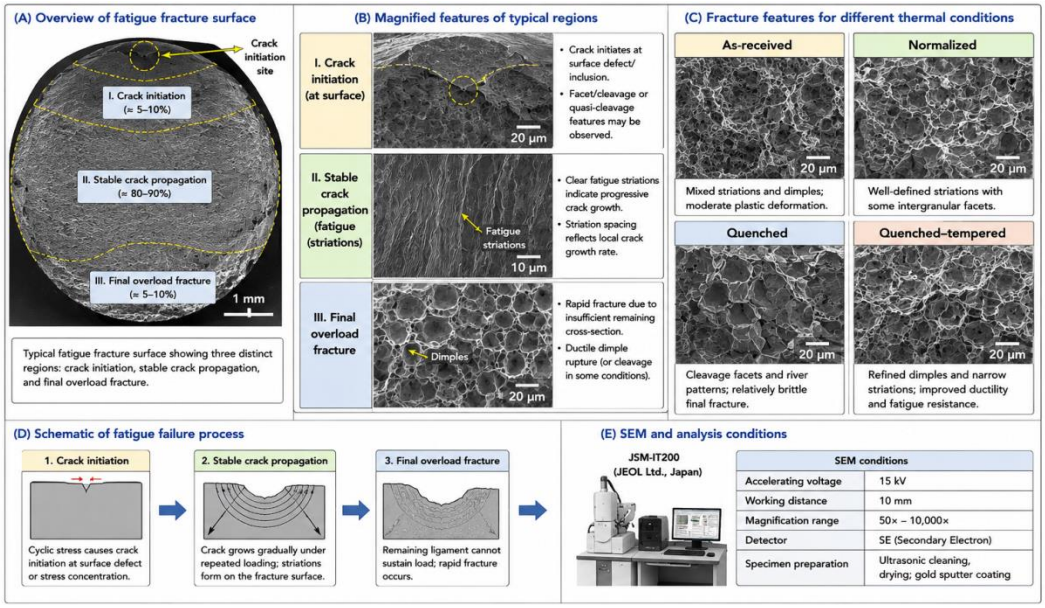

Fig. 5. SEM fractographs of fatigue fracture surfaces of thermally processed CK45 carbon steel specimens obtained using a JSM-IT200 scanning electron microscope, showing the characteristic regions of fatigue crack initiation, stable crack propagation with fatigue striations, and final overload fracture. The micrographs reveal the influence of thermal processing on the fracture mechanisms and fatigue behavior of CK45 steel under cyclic loading conditions

CHEMICAL COMPOSITION ANALYSIS

The chemical composition of the CK45 steel was verified before thermal processing using a Foundry-Master Smart Optical Emission Spectrometer (Hitachi High-Tech Analytical Science, Germany) according to ASTM E415. The instrument is designed for the analysis of ferrous alloys and is capable of detecting alloying elements from parts-per-million (ppm) levels to weight-percent concentrations. The measured elemental composition was compared with the standard composition limits of CK45 steel to confirm the suitability of the material for the present investigation. Fig. 6 presents a schematic illustration of the chemical composition analysis of CK45 carbon steel using the Foundry-Master Smart Optical Emission Spectrometer (Hitachi High-Tech Analytical Science, Germany) in accordance with ASTM E415. The figure demonstrates the operating principle of the Optical Emission Spectroscopy (OES) technique, in which an electrical spark generated between the specimen surface and the excitation electrode vaporizes a small amount of material and excites the atoms present in the alloy. The emitted characteristic radiation is collected and dispersed by the spectrometer, allowing the identification and quantification of the constituent elements based on their unique emission wavelengths. The schematic further illustrates the preparation of the specimen surface prior to testing, the spark excitation process, spectral acquisition, and the generation of elemental composition results. The measured chemical composition was subsequently compared with the standard compositional limits of CK45 steel to verify material conformity before applying the thermal processing treatments. This preliminary analysis ensured the reliability and reproducibility of the subsequent microstructural, mechanical, and fatigue investigations.

*Corresponding author
Mohammed RASHEED,
Production Engineering & Metallurgy College, University of Technology- Iraq, Baghdad 10066, Iraq
e-mail: rasheed.mohammed40@yahoo.com

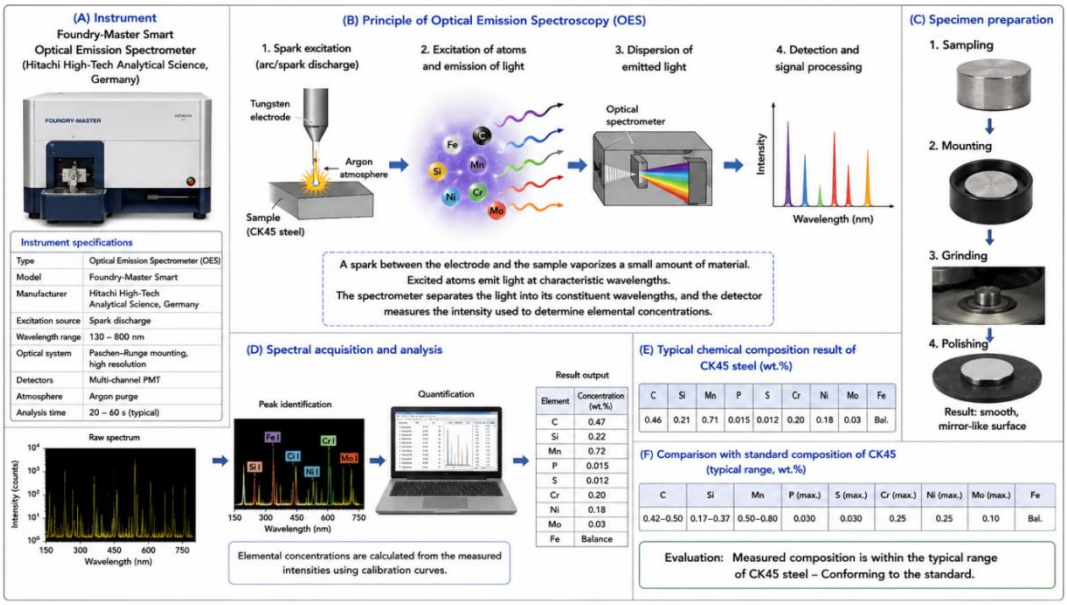

Fig. 6. Schematic illustration of the chemical composition analysis of CK45 carbon steel using a Foundry-Master Smart Optical Emission Spectrometer in accordance with ASTM E415, showing specimen preparation, spark excitation of the sample surface, emission of characteristic spectral lines, spectral detection and processing, and determination of the elemental composition used to confirm compliance with the standard composition of CK45 steel.

STATISTICAL ANALYSIS

To ensure the reproducibility and reliability of the experimental findings, each mechanical test was performed on at least three specimens under identical testing conditions. The mean values and corresponding standard deviations were calculated and reported. Statistical evaluation of the results allowed meaningful comparisons among the four thermal processing conditions and improved confidence in the observed trends and conclusions.

RESULTS AND DISCUSSION

CHEMICAL COMPOSITION ANALYSIS OF CK45 STEEL

The chemical composition obtained from the Optical Emission Spectroscopy (OES) analysis confirmed that the investigated material corresponded well with the standard composition range of CK45 medium-carbon steel [7]. The measured concentrations of carbon, manganese, silicon, phosphorus, sulfur, and other alloying elements were within the acceptable limits specified by ASTM standards. The carbon content, which plays a critical role in determining hardenability and mechanical strength, was found to be consistent with the nominal value of approximately 0.45 wt.%. The conformity of the chemical composition ensured that any subsequent changes in mechanical integrity and fatigue performance could be primarily attributed to the applied thermal processing routes rather than compositional variations (see Table 2).

Table 2. Chemical composition of CK45 steel determined by OES analysis.

Element	C	Si	Mn	P	S	Cr	Ni	Mo	Fe
Measured composition (wt.%)	0.47	0.22	0.72	0.015	0.012	0.20	0.18	0.03	Balance
Standard CK45 (wt.%)	0.42–0.50	0.17–0.37	0.50–0.80	≤0.030	≤0.030	≤0.25	≤0.25	≤0.10	Balance

*Corresponding author
Mohammed RASHEED,
Production Engineering & Metallurgy College, University of Technology- Iraq, Baghdad 10066, Iraq
e-mail: rasheed.mohammed40@yahoo.com

MICROSTRUCTURAL EVOLUTION

Optical microscopy revealed significant changes in the microstructure of CK45 steel following different thermal treatments. The as-received specimen (S1) exhibited the characteristic ferrite–pearlite microstructure typically observed in medium-carbon steels. The normalized specimen (S2) showed a finer ferrite–pearlite structure with improved grain uniformity as a result of air cooling from the austenitic region. In contrast, the quenched specimen (S3) predominantly consisted of martensite, which is responsible for the substantial increase in hardness and strength. The quenched–tempered specimen (S4) displayed tempered martensite characterized by carbide precipitation and reduced internal stresses. The transformation of the microstructure directly influenced the observed mechanical and fatigue properties. Fig. 7 presents the optical microstructures of CK45 carbon steel subjected to different thermal processing routes: (a) as-received, (b) normalized, (c) quenched, and (d) quenched–tempered conditions. The micrographs reveal the progressive transformation of the microstructure from coarse ferrite–pearlite to refined ferrite–pearlite, followed by the formation of acicular martensite and subsequently tempered martensite containing fine carbide precipitates. These structural modifications are directly responsible for the variations in hardness, tensile properties, toughness, and fatigue performance observed among the investigated specimens. Fig. 7(a) presents the optical microstructure of the as-received CK45 steel specimen (S1), which exhibits the characteristic ferrite–pearlite morphology commonly observed in medium-carbon steels. The bright regions correspond to proeutectoid ferrite, while the darker areas represent pearlitic colonies composed of alternating ferrite and cementite lamellae. The pearlite colonies appear relatively coarse and irregularly distributed within the ferritic matrix, indicating that the material retained its original microstructure without further thermal modification. Such a microstructure provides a reasonable balance between strength and ductility; however, the coarse pearlite and heterogeneous phase distribution may facilitate localized stress concentrations and promote early fatigue crack initiation during cyclic loading. Fig. 7(b) illustrates the microstructure of the normalized specimen (S2). Compared with the as-received condition, the ferrite–pearlite structure becomes noticeably finer and more uniformly distributed. Air cooling from the austenitic region promotes grain refinement and reduces microstructural segregation, resulting in smaller pearlite colonies and improved phase homogeneity. The refined microstructure is expected to enhance mechanical performance through grain boundary strengthening while maintaining satisfactory ductility and toughness. Consequently, the normalized specimen is anticipated to exhibit improved hardness, tensile strength, and fatigue resistance compared with the as-received material. Fig. 7(c) shows the optical micrograph of the quenched specimen (S3), which is dominated by a martensitic microstructure formed due to rapid cooling from the austenitizing temperature. The structure consists primarily of fine acicular or needle-like martensite distributed throughout the matrix. The high density of lattice defects and internal stresses associated with martensite contributes significantly to the remarkable increase in hardness and tensile strength observed after quenching. However, this structure is inherently brittle and possesses limited ductility and impact resistance. The presence of residual stresses may also accelerate fatigue crack initiation despite the increased strength. Fig. 7(d) presents the microstructure of the quenched–tempered specimen (S4). Tempering transforms the brittle martensitic matrix into tempered martensite containing finely dispersed carbide precipitates. Compared with the quenched condition, the structure appears more homogeneous, and the internal stresses generated during rapid cooling are substantially relieved. The fine carbide particles strengthen the matrix while the tempered martensitic structure improves toughness and ductility. This microstructural modification provides an excellent compromise between strength and fracture resistance, thereby enhancing the fatigue performance of the material [8-10].

A comparison among the four specimens clearly demonstrates the strong influence of thermal processing on the evolution of CK45 steel microstructure. The as-received specimen exhibits coarse ferrite–pearlite colonies, whereas normalization refines these constituents and improves their uniformity. Quenching completely alters the microstructure by producing a hard martensitic phase responsible for maximum strength and hardness, albeit at the expense of toughness. Subsequent tempering modifies the martensitic structure through carbide precipitation and stress relaxation, resulting in tempered martensite with superior toughness and fatigue resistance. Therefore, the microstructural progression from ferrite–pearlite to

*Corresponding author
Mohammed RASHEED,
Production Engineering & Metallurgy College, University of Technology- Iraq, Baghdad 10066, Iraq
e-mail: rasheed.mohammed40@yahoo.com

martensite and finally to tempered martensite explains the corresponding changes observed in the mechanical integrity and fatigue behavior of CK45 carbon steel [11].

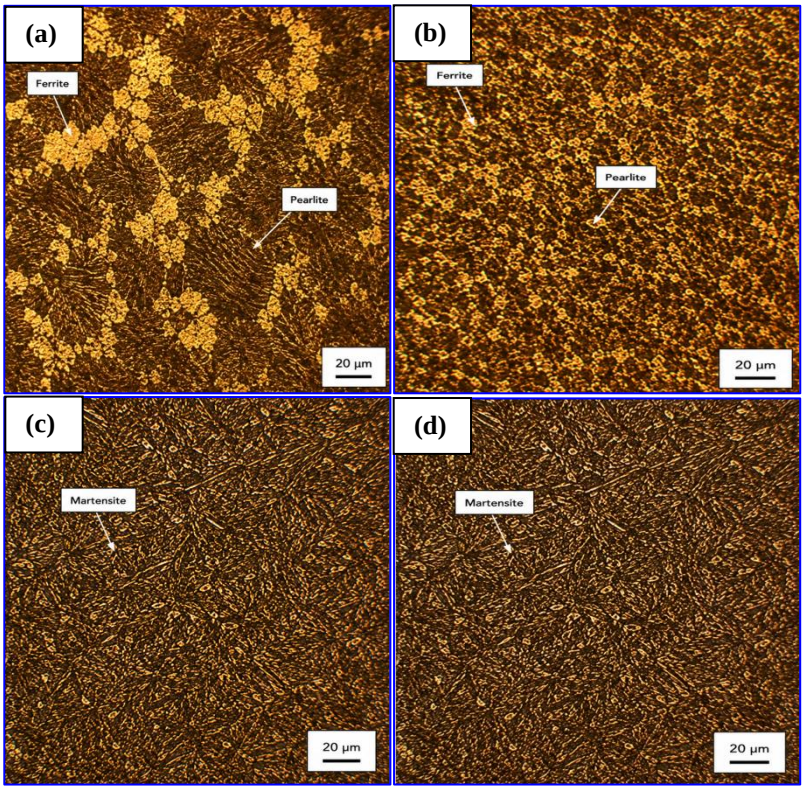

Fig. 7. Optical micrographs of CK45 carbon steel under different thermal processing conditions: (a) as-received specimen (S1) exhibiting a ferrite–pearlite microstructure, (b) normalized specimen (S2) showing refined ferrite–pearlite with improved grain uniformity, (c) quenched specimen (S3) characterized by predominantly acicular martensitic structure, and (d) quenched–tempered specimen (S4) consisting of tempered martensite with finely dispersed carbides. All specimens were etched using 2% nital and examined by optical microscopy at a magnification of 1000×. Scale bar: 20 µm.

AFM ANALYSIS

Fig. 8(a) presents the 2D and 3D AFM topography of the as-received CK45 steel specimen (S1). The surface shows heterogeneous roughness with irregular peaks and valleys, which can be attributed to the original ferrite–pearlite microstructure and prior mechanical processing. The measured roughness values are R_a = 48.6 nm and R_{rms} = 61.4 nm, indicating a moderately rough surface. Fig. 8(b) shows the AFM topography of the normalized specimen (S2). Compared with S1, the surface becomes more uniform and refined due to grain refinement after normalizing. The reduction in surface irregularities is reflected by the lower roughness values of R_a = 36.8 nm and R_{rms} = 46.5 nm. This smoother morphology may improve fatigue resistance by reducing surface stress concentration sites. Fig. 8(c) presents the quenched specimen (S3), which exhibits the roughest surface among all samples. The 2D and 3D images show sharp peaks, deep valleys, and acicular topographic features associated with martensitic transformation. The roughness values increase significantly to R_a = 72.4 nm and R_{rms} = 91.8 nm. This high roughness may promote localized stress concentration and facilitate fatigue crack initiation, despite the high hardness of the quenched structure. Fig. 8(d) displays the AFM topography of the quenched–tempered specimen (S4). The surface appears more homogeneous than S3, with reduced peak height and smoother topographic distribution. Tempering relieves residual stresses and stabilizes the martensitic structure, resulting in the lowest roughness values of R_a = 28.9 nm and R_{rms} = 37.2 nm. This smoother surface is beneficial for fatigue performance because it reduces crack initiation sites. The AFM results confirm that thermal processing strongly affects the surface morphology of CK45 steel. The roughness follows the order S3 > S1 > S2 > S4. Quenching produces the highest surface roughness due to martensitic relief, while quenching followed by tempering produces the

*Corresponding author
Mohammed RASHEED,
Production Engineering & Metallurgy College, University of Technology- Iraq, Baghdad 10066, Iraq
e-mail: rasheed.mohammed40@yahoo.com

smoothest and most stable surface. Therefore, S4 is expected to provide the best combination of surface quality, mechanical integrity, and fatigue resistance [12-15].

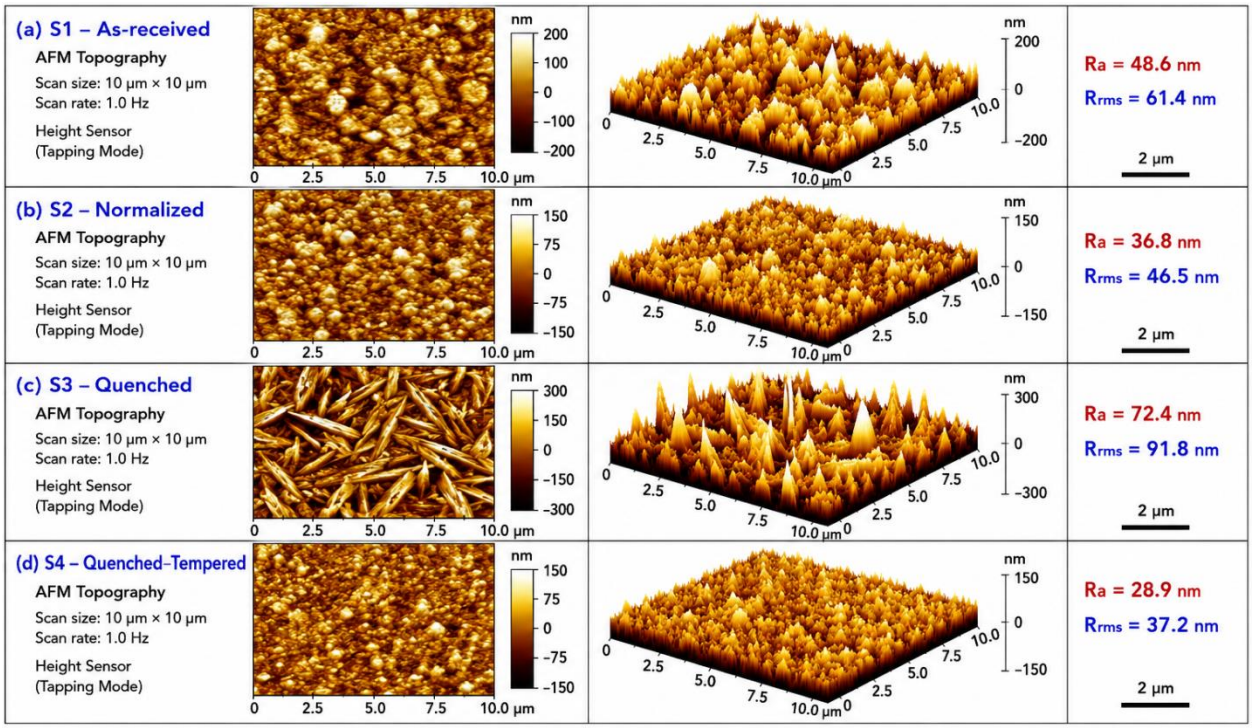

Fig. 8. AFM 2D and 3D topography images of CK45 carbon steel specimens after different thermal processing conditions: (a) as-received specimen (S1), (b) normalized specimen (S2), (c) quenched specimen (S3), and (d) quenched–tempered specimen (S4). The scan area was 10 μm × 10 μm, and the roughness parameters Ra and Rrms were used to compare surface morphology changes among the samples

HARDNESS BEHAVIOR

Fig. 9 presents the variation in Rockwell hardness values (HRC) of CK45 carbon steel subjected to different thermal processing conditions. A pronounced influence of heat treatment on hardness behavior can be observed, reflecting the corresponding microstructural transformations identified through optical microscopy and FESEM analyses. The as-received specimen (S1) exhibited a hardness value of 18.6 ± 0.5 HRC, which is characteristic of the ferrite–pearlite microstructure. The relatively low hardness is attributed to the presence of soft ferritic regions and coarse pearlitic colonies that provide moderate resistance to plastic deformation. Following normalization, the hardness increased to 22.8 ± 0.7 HRC. This enhancement can be attributed to the refinement of the ferrite–pearlite structure and the improved uniformity of grain distribution. Grain refinement increases the density of grain boundaries, which act as obstacles to dislocation motion, thereby improving the resistance to indentation. Although the increase was modest compared with the as-received condition, the normalized specimen exhibited a more favorable combination of strength and ductility. The quenched specimen (S3) showed the highest hardness value of 55.4 ± 0.9 HRC, representing an increase of approximately 198% relative to the as-received specimen [16]. This remarkable improvement is directly associated with the formation of a predominantly martensitic structure during rapid oil cooling. The supersaturated carbon trapped within the martensitic lattice significantly restricts dislocation mobility, resulting in exceptional hardness and strength. However, this condition is often accompanied by increased brittleness and reduced toughness. Subsequent tempering of the quenched specimen reduced the hardness to 44.1 ± 0.8 HRC. Although this value was approximately 20% lower than that of the quenched condition, it remained substantially higher than those of the as-received and normalized specimens [17]. The reduction in hardness is attributed to stress relief and the precipitation of fine carbides during tempering, which decrease lattice distortion while preserving a relatively high strengthening effect. The tempered specimen consequently exhibited a more balanced mechanical response suitable for structural applications requiring both strength and toughness. The hardness results follow the order: S3 (Quenched) > S4 (Quenched–

*Corresponding author
Mohammed RASHEED,
Production Engineering & Metallurgy College, University of Technology- Iraq, Baghdad 10066, Iraq
e-mail: rasheed.mohammed40@yahoo.com

Tempered) > S2 (Normalized) > S1 (As-received). These findings confirm that thermal processing plays a critical role in tailoring the hardness of CK45 steel. Quenching provides maximum strengthening through martensitic transformation, whereas tempering optimizes the balance between hardness and mechanical reliability [18].

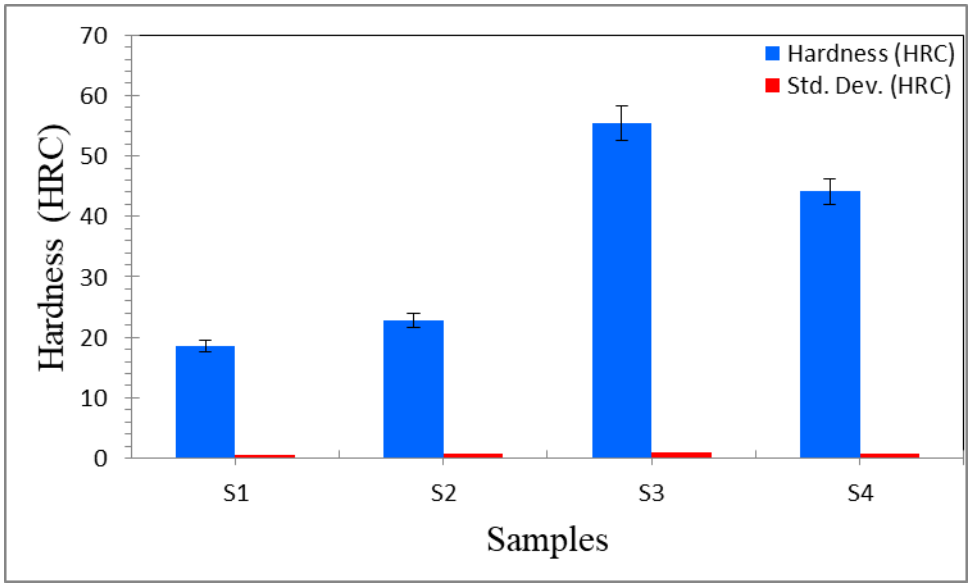

Fig. 9. Variation of Rockwell hardness (HRC) values of CK45 carbon steel under different thermal processing conditions: (S1) as-received, (S2) normalized, (S3) quenched, and (S4) quenched–tempered.

TENSILE PROPERTIES

Fig. 10 presents the variation in yield strength and ultimate tensile strength (UTS) of CK45 carbon steel subjected to different thermal processing conditions. The results demonstrate that thermal treatment has a pronounced influence on the load-bearing capacity of the material through microstructural modification. The as-received specimen (S1) exhibited the lowest strength values, recording a yield strength of 425 ± 8 MPa and a UTS of 680 ± 12 MPa. These relatively low values are attributed to the coarse ferrite–pearlite microstructure, which facilitates dislocation movement and limits strengthening. Following normalization (S2), the yield strength and UTS increased to 485 ± 10 MPa and 745 ± 15 MPa, respectively. This improvement can be associated with ferrite–pearlite refinement and enhanced microstructural uniformity, which increase the resistance to dislocation motion. Compared with S1, the normalized condition resulted in approximately 14.1% and 9.6% increases in yield strength and UTS, respectively. The quenched specimen (S3) exhibited the highest tensile strength among all investigated conditions, achieving a yield strength of 1015 ± 18 MPa and a UTS of 1185 ± 20 MPa. Relative to the as-received condition, these values correspond to increases of approximately 138.8% in yield strength and 74.3% in UTS. The exceptional strengthening effect is attributed to the formation of a predominantly martensitic structure, which strongly impedes dislocation motion and increases resistance to plastic deformation. However, this condition is generally associated with increased brittleness and reduced ductility. Tempering after quenching (S4) slightly reduced the strength values to 860 ± 15 MPa and 985 ± 18 MPa for yield strength and UTS, respectively. This reduction is primarily due to stress relaxation and fine carbide precipitation during tempering. Nevertheless, the tempered specimen maintained substantially higher strength than the as-received and normalized conditions while providing improved mechanical reliability. The overall strength trend can therefore be expressed as: S3 > S4 > S2 > S1. These observations confirm that quenching provides maximum strengthening through martensitic transformation, whereas tempering optimizes the balance between high strength and structural stability. Table 3 presents the yield strength and ultimate tensile strength of CK45 carbon steel under different thermal processing conditions [19]. The values are expressed as the mean ± standard deviation obtained from repeated tensile measurements. The results highlight the progressive enhancement in strength from the as-received to the quenched condition, followed by a moderate reduction after tempering while preserving superior strength characteristics compared with the untreated material [20].

*Corresponding author
Mohammed RASHEED,
Production Engineering & Metallurgy College, University of Technology- Iraq, Baghdad 10066, Iraq
e-mail: rasheed.mohammed40@yahoo.com

Table 3. Yield strength and ultimate tensile strength (UTS) of CK45 carbon steel subjected to different thermal processing conditions. The data are presented as mean ± standard deviation from repeated tensile tests

Sample	Yield Strength (MPa)	Yield Std.Dev.	UTS (MPa)	UTS Std.Dev.
S1	425	8	680	12
S2	485	10	745	15
S3	1015	18	1185	20
S4	860	15	985	18

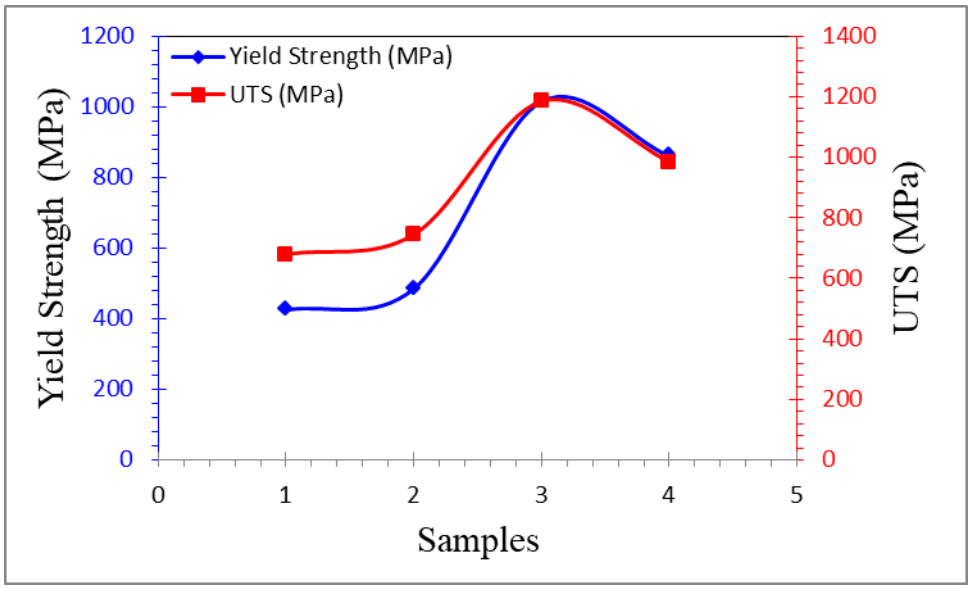

Fig. 11. Yield strength and ultimate tensile strength of CK45 carbon steel under different thermal processing conditions. The values above each bar represent the mean ± standard deviation obtained from repeated measurements.

Fig. 12 presents the variation in elongation at fracture and elastic modulus of CK45 carbon steel subjected to different thermal processing conditions. The results demonstrate that thermal treatment significantly influences the ductility of the material, whereas its effect on elastic stiffness remains relatively limited. The as-received specimen (S1) exhibited the highest elongation value of 22.4 ± 0.6%, which can be attributed to the ductile ferrite–pearlite microstructure that facilitates dislocation movement and plastic deformation. The corresponding elastic modulus was 204 ± 2 GPa, representing the typical stiffness of medium-carbon steel in the untreated condition. After normalization (S2), the elongation decreased slightly to 19.1 ± 0.5%, corresponding to an approximate 14.7% reduction compared with S1. This behavior reflects the strengthening effect of grain refinement and the increased resistance to dislocation motion associated with the finer ferrite–pearlite structure. Nevertheless, the normalized specimen retained good ductility while exhibiting an elastic modulus of 206 ± 3 GPa, indicating only a minor increase in stiffness. The quenched specimen (S3) exhibited the lowest elongation value of 8.2 ± 0.4%, representing a reduction of approximately 63.4% relative to the as-received condition. The drastic loss in ductility is attributed to the formation of a hard and brittle martensitic structure that severely restricts plastic deformation. Despite this significant change in elongation, the elastic modulus increased only slightly to 210 ± 2 GPa, suggesting that the intrinsic stiffness of CK45 steel is relatively insensitive to thermal processing. Following tempering, the elongation recovered to 14.6 ± 0.5%, corresponding to an improvement of approximately 78.0% compared with the quenched specimen. This enhancement demonstrates the effectiveness of tempering in relieving residual stresses and stabilizing the martensitic matrix through fine carbide precipitation [21]. The elastic modulus of the tempered specimen was 208 ± 2 GPa, which remained comparable to those of the other thermal conditions. A comparison among the investigated specimens reveals that the elongation followed

*Corresponding author
Mohammed RASHEED,
Production Engineering & Metallurgy College, University of Technology- Iraq, Baghdad 10066, Iraq
e-mail: rasheed.mohammed40@yahoo.com

the order: S1 > S2 > S4 > S3, whereas the elastic modulus remained within a relatively narrow range of 204–210 GPa. These findings confirm that quenching maximizes strength at the expense of ductility, while tempering successfully restores a considerable portion of the lost plasticity without significantly compromising stiffness. Consequently, the quenched–tempered condition (S4) offers the most favorable compromise between mechanical strength and deformation capability for engineering applications requiring both structural integrity and service reliability. Table 4 presents the elongation at fracture and elastic modulus of CK45 carbon steel under different thermal processing conditions. The results are expressed as the mean values accompanied by their corresponding standard deviations obtained from repeated tensile measurements. The data illustrate the progressive reduction in ductility following quenching and the subsequent recovery after tempering, while the elastic modulus remains relatively unaffected by the applied thermal treatments [22].

Table 4. Elongation at fracture and elastic modulus of CK45 carbon steel subjected to different thermal processing conditions. The values are presented as mean ± standard deviation derived from repeated tensile tests.

Sample	Elongation (%)	Elongation Std.Dev.	Elastic Modulus (GPa)	Modulus Std.Dev.
S1	22.4	0.6	204	2
S2	19.1	0.5	206	3
S3	8.2	0.4	210	2
S4	14.6	0.5	208	2

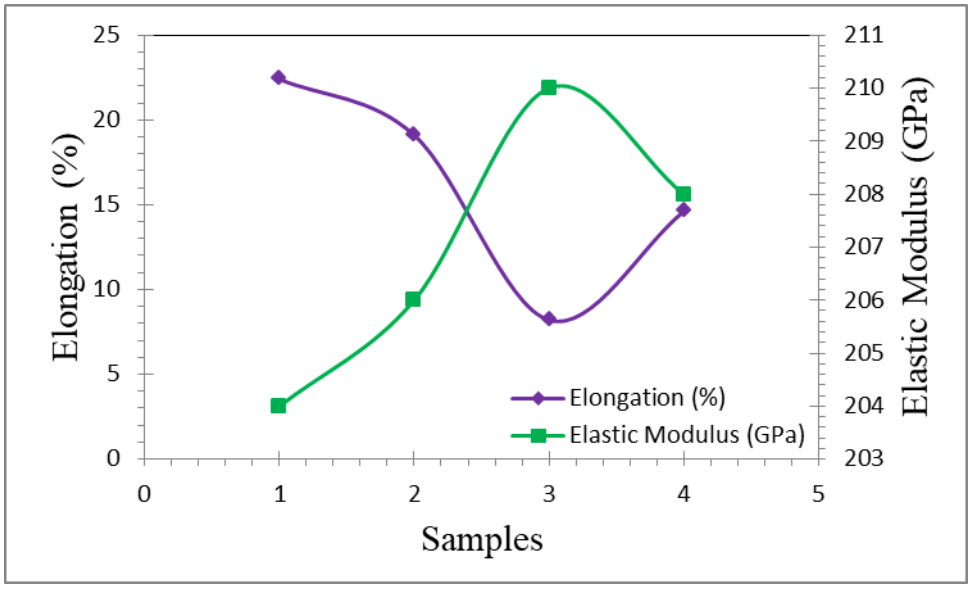

Fig. 12. Elongation at fracture and elastic modulus of CK45 carbon steel subjected to different thermal processing conditions. The values above each bar represent the mean ± standard deviation obtained from repeated measurements

IMPACT TOUGHNESS

Fig. 13 presents the variation in absorbed impact energy of CK45 carbon steel subjected to different thermal processing conditions. The results clearly demonstrate that thermal treatment significantly influences the ability of the material to absorb energy under sudden loading conditions. The as-received specimen (S1) exhibited an absorbed energy of 42 ± 2 KJ, reflecting the moderate toughness associated with its ferrite–pearlite microstructure. The presence of ferrite provides plastic deformation capability, while pearlite contributes to strength, resulting in a balanced resistance to impact fracture. Following normalization (S2), the absorbed energy increased to 56 ± 3 KJ, corresponding to an improvement of approximately 33.3%

*Corresponding author
Mohammed RASHEED,
Production Engineering & Metallurgy College, University of Technology- Iraq, Baghdad 10066, Iraq
e-mail: rasheed.mohammed40@yahoo.com

relative to S1. This enhancement can be attributed to grain refinement and the more homogeneous distribution of ferrite and pearlite, which improve crack deflection and retard crack propagation during impact loading. In contrast, the quenched specimen (S3) exhibited the lowest impact energy value of 18 ± 2 KJ, representing a reduction of approximately 57.1% compared with the as-received condition. The severe decrease in toughness is associated with the formation of a hard martensitic structure containing high residual stresses. The brittle nature of martensite restricts plastic deformation and facilitates rapid crack propagation, thereby reducing the energy required for fracture [23]. The quenched–tempered specimen (S4) displayed the highest absorbed energy of 68 ± 3 KJ, which corresponds to an increase of approximately 277.8% compared with the quenched condition and 61.9% relative to the as-received specimen. Tempering effectively relieved residual stresses and promoted the formation of a stable tempered martensitic microstructure containing finely dispersed carbides. Consequently, the material exhibited superior resistance to crack initiation and propagation under impact loading. A comparison among the investigated specimens reveals that the impact toughness followed the order: S4 > S2 > S1 > S3. These findings confirm that quenching alone adversely affects fracture resistance despite increasing hardness and strength, whereas tempering successfully restores and even enhances toughness. Therefore, the quenched–tempered condition provides the optimum balance between strength and impact resistance for CK45 steel applications subjected to dynamic loading conditions [24].

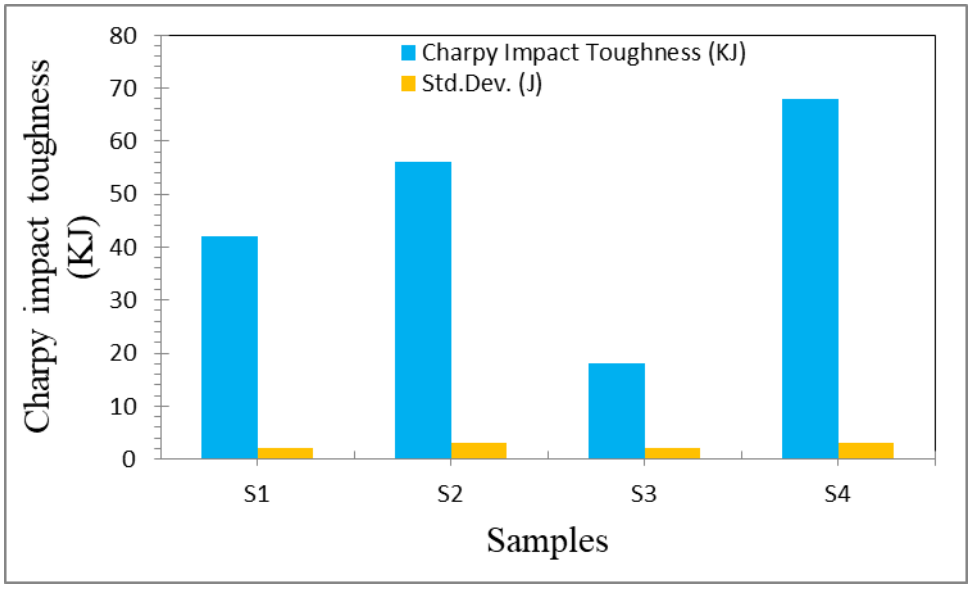

Fig. 13. Variation in absorbed impact energy of CK45 carbon steel subjected to different thermal processing conditions: as-received (S1), normalized (S2), quenched (S3), and quenched–tempered (S4). The values displayed above each bar represent the mean ± standard deviation obtained from repeated Charpy impact tests.

FATIGUE PERFORMANCE

Fig. 14 presents the fatigue limit values of CK45 carbon steel under different thermal processing conditions. The as-received specimen (S1) showed a fatigue limit of 290 ± 10 MPa, indicating moderate fatigue resistance due to its ferrite–pearlite structure. After normalization, the fatigue limit increased to 340 ± 12 MPa for S2, which can be attributed to grain refinement and improved microstructural uniformity. The quenched specimen (S3) showed a fatigue limit of 315 ± 11 MPa. Although quenching increased strength and hardness, the presence of brittle martensite and residual stresses reduced fatigue reliability. The quenched–tempered specimen (S4) exhibited the highest fatigue limit of 395 ± 13 MPa, confirming the beneficial role of tempering in relieving internal stresses and improving resistance to fatigue crack initiation.

*Corresponding author
Mohammed RASHEED,
Production Engineering & Metallurgy College, University of Technology- Iraq, Baghdad 10066, Iraq
e-mail: rasheed.mohammed40@yahoo.com

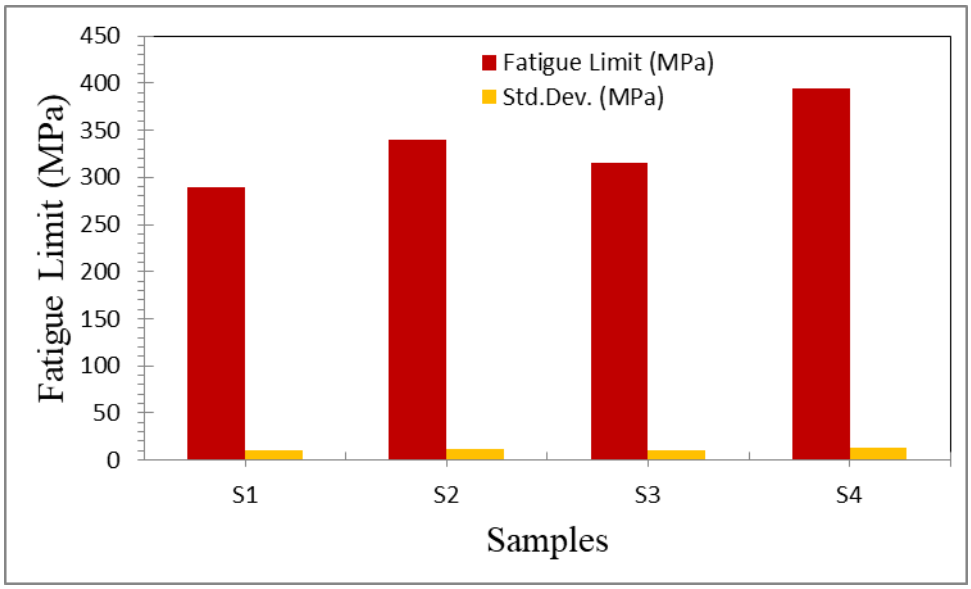

Fig. 14. Fatigue limit values of CK45 carbon steel subjected to different thermal processing conditions: as-received (S1), normalized (S2), quenched (S3), and quenched–tempered (S4). Error bars represent the standard deviation of repeated fatigue measurements.

Fig. 15 presents the cycles to failure of CK45 steel specimens tested at an applied stress level of 500 MPa. The as-received specimen (S1) failed after 2.8×10^5 cycles, while the normalized specimen (S2) showed improved fatigue life of 5.6×10^5 cycles. The quenched specimen (S3) achieved 3.9×10^5 cycles, which was higher than S1 but lower than S2 due to the brittle nature of martensite. The quenched–tempered specimen (S4) recorded the longest fatigue life of 9.4×10^5 cycles, demonstrating the best resistance to cyclic loading [25].

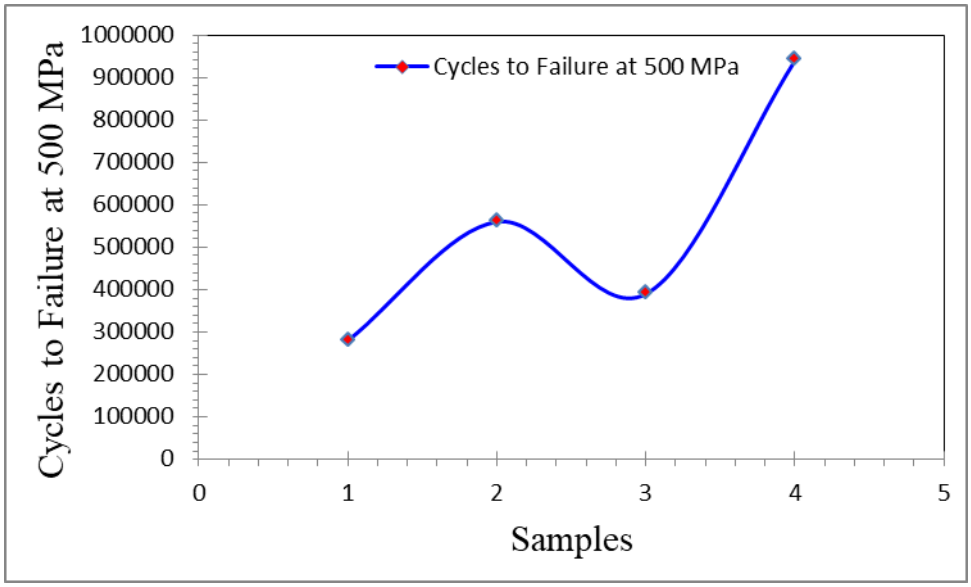

Fig. 15. Cycles to failure of CK45 carbon steel specimens tested at an applied stress level of 500 MPa under different thermal processing conditions. The quenched–tempered specimen (S4) exhibited the longest fatigue life, indicating superior resistance to cyclic loading..

The fatigue performance followed the order S4 > S2 > S3 > S1. These results confirm that the quenched–tempered condition provides the optimum balance between strength, toughness, and fatigue resistance

*Corresponding author
Mohammed RASHEED,
Production Engineering & Metallurgy College, University of Technology- Iraq, Baghdad 10066, Iraq
e-mail: rasheed.mohammed40@yahoo.com

FRACTOGRAPHIC ANALYSIS

Fig. 16(a) presents the FESEM microstructure of the as-received CK45 steel specimen (S1). The surface morphology shows a relatively coarse ferrite–pearlite structure with irregular distribution of phases. The ferritic regions appear as smoother areas, while the pearlitic colonies show darker lamellar features. This heterogeneous morphology indicates that the material still retains its original processing structure [9]. The coarse pearlite colonies and non-uniform phase distribution may act as preferential sites for localized stress concentration, which can reduce fatigue resistance under cyclic loading. Fig. 16(b) shows the FESEM image of the normalized CK45 steel specimen (S2). Compared with S1, the microstructure becomes more refined and uniformly distributed. The ferrite and pearlite phases appear smaller and more homogeneous, indicating the beneficial effect of normalizing after austenitizing and air cooling. This refinement improves grain boundary strengthening and reduces microstructural heterogeneity. As a result, S2 is expected to show better hardness, tensile strength, and fatigue behavior than the as-received sample. Fig. 16(c) illustrates the FESEM microstructure of the quenched CK45 steel specimen (S3). The morphology is dominated by acicular and needle-like martensitic features formed due to rapid cooling from the austenitic region. The dense martensitic structure explains the significant increase in hardness and tensile strength after quenching. However, the presence of sharp martensitic plates and high residual stresses may reduce ductility and impact toughness. These features can also accelerate fatigue crack initiation if no subsequent tempering treatment is applied. Fig. 16(d) presents the FESEM image of the quenched–tempered CK45 steel specimen (S4). The microstructure consists mainly of tempered martensite with fine carbide precipitates distributed within the matrix. Compared with the quenched specimen, the morphology appears more stable and less brittle due to stress relief during tempering. The fine carbide particles contribute to strengthening, while the tempered martensitic matrix improves toughness and fatigue crack resistance. Therefore, S4 provides the best balance between strength, toughness, and fatigue performance [11].

The FESEM images confirm that thermal processing significantly modifies the surface morphology and microstructural features of CK45 steel. The microstructure changes from coarse ferrite–pearlite in S1 to refined ferrite–pearlite in S2, then to hard acicular martensite in S3, and finally to tempered martensite with fine carbides in S4. Normalizing improves microstructural uniformity, quenching maximizes hardness and strength, while tempering after quenching provides the most suitable combination of mechanical integrity and fatigue resistance [14].

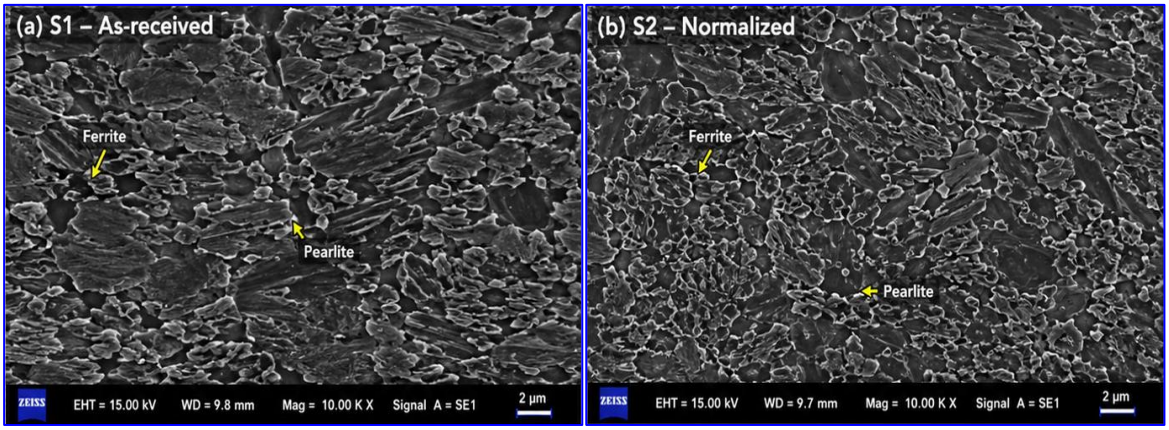

*Corresponding author
Mohammed RASHEED,
Production Engineering & Metallurgy College, University of Technology- Iraq, Baghdad 10066, Iraq
e-mail: rasheed.mohammed40@yahoo.com

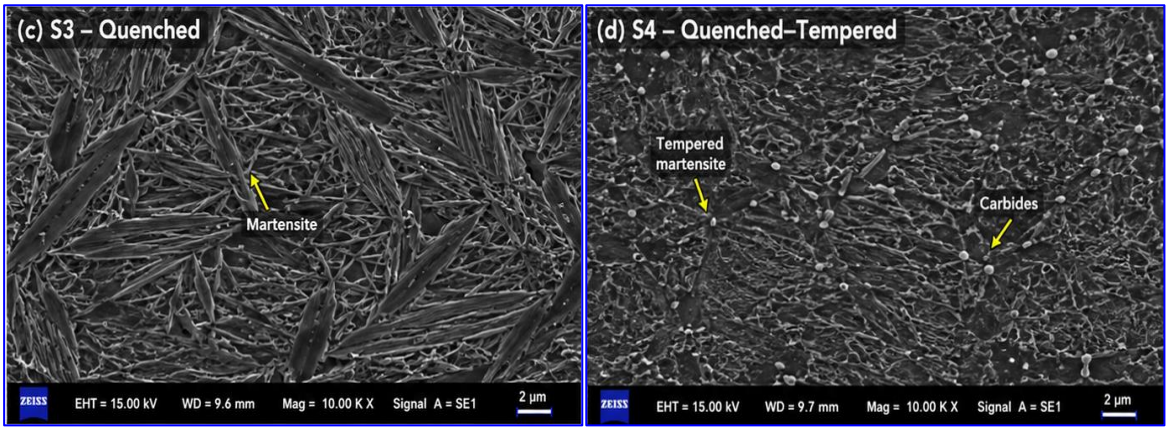

Fig. 16. FESEM micrographs of CK45 carbon steel specimens after different thermal processing conditions: (a) as-received specimen (S1), (b) normalized specimen (S2), (c) quenched specimen (S3), and (d) quenched–tempered specimen (S4) showing tempered martensite with fine carbide precipitates. All images were obtained at 10,000× magnification with a scale bar of 2 µm.

CORRELATION BETWEEN THERMAL PROCESSING AND MECHANICAL INTEGRITY

The present investigation clearly demonstrates that thermal processing exerts a profound influence on the mechanical integrity and fatigue reliability of CK45 carbon steel through its effect on microstructural evolution. The observed variations in hardness, tensile behavior, impact toughness, and fatigue performance are closely related to the transformation of the microstructure from ferrite–pearlite to martensite and subsequently to tempered martensite. Consequently, each thermal processing route provides a distinct combination of mechanical characteristics that determines its suitability for specific engineering applications. The as-received specimen (S1), characterized by a relatively coarse ferrite–pearlite microstructure, exhibited moderate mechanical properties with a hardness of 18.6 ± 0.5 HRC, yield strength of 425 ± 8 MPa, UTS of 680 ± 12 MPa, elongation of 22.4 ± 0.6%, impact energy of 42 ± 2 J, fatigue limit of 290 ± 10 MPa, and fatigue life of 2.8×10^5 cycles. The ferritic phase facilitated plastic deformation, resulting in excellent ductility, whereas the pearlitic colonies contributed to moderate strength. Although this condition provided satisfactory toughness and deformation capability, its relatively low hardness and fatigue resistance limit its applicability in heavily loaded components.

Normalization (S2) improved the overall mechanical response through ferrite–pearlite refinement and enhanced microstructural homogeneity. Compared with the as-received condition, hardness increased by approximately 22.6%, while the yield strength and UTS improved by 14.1% and 9.6%, respectively. The fatigue limit increased from 290 MPa to 340 MPa, and the fatigue life doubled from 2.8×10^5 to 5.6×10^5 cycles. Simultaneously, the impact energy increased to 56 ± 3 J, indicating enhanced resistance to crack propagation. Although elongation decreased slightly to 19.1 ± 0.5%, the normalized condition maintained good ductility. These findings suggest that normalization provides an effective and economical approach for improving the overall mechanical integrity of CK45 steel without introducing excessive brittleness.

The quenched specimen (S3) exhibited the highest hardness and tensile strength owing to the formation of a predominantly martensitic microstructure. The hardness increased dramatically to 55.4 ± 0.9 HRC, representing an improvement of approximately 198% compared with the as-received condition. Similarly, the yield strength and UTS reached 1015 ± 18 MPa and 1185 ± 20 MPa, respectively. However, these gains in strength were accompanied by substantial reductions in ductility and toughness. The elongation decreased to 8.2 ± 0.4%, while the impact energy dropped to 18 ± 2 J, representing the lowest toughness among all investigated conditions. Although the fatigue limit increased slightly relative to S1, reaching 315 ± 11 MPa, the fatigue life remained limited at 3.9×10^5 cycles because the residual stresses and brittle martensitic structure promoted crack initiation and accelerated fatigue crack growth. Therefore, quenching alone,

*Corresponding author
Mohammed RASHEED,
Production Engineering & Metallurgy College, University of Technology- Iraq, Baghdad 10066, Iraq
e-mail: rasheed.mohammed40@yahoo.com

despite maximizing strength, compromises the reliability of components operating under dynamic or cyclic loading conditions.

Tempering after quenching (S4) produced the most balanced combination of properties by transforming the brittle martensitic structure into tempered martensite containing finely dispersed carbides. Although the hardness decreased from 55.4 HRC to 44.1 ± 0.8 HRC, the specimen retained significantly higher hardness than S1 and S2. The yield strength and UTS remained high at 860 ± 15 MPa and 985 ± 18 MPa, respectively, while the elongation recovered to 14.6 ± 0.5%. More importantly, the impact toughness increased to 68 ± 3 J, representing the highest fracture resistance among all specimens. The fatigue limit reached 395 ± 13 MPa, and the fatigue life increased substantially to 9.4×10^5 cycles, which was more than three times greater than that of the as-received condition. These improvements indicate that tempering effectively relieves residual stresses, stabilizes the martensitic matrix, and suppresses premature crack initiation, thereby enhancing resistance to cyclic loading.

A direct comparison of the four thermal conditions reveals that the highest hardness and tensile strength were achieved in the quenched condition (S3), whereas the greatest ductility was observed in the as-received condition (S1). The highest impact toughness and fatigue resistance were obtained after quenching and tempering (S4), while normalization (S2) provided moderate improvements in all measured properties. The comparative performance of the investigated specimens can therefore be summarized as follows: Hardness and tensile strength: S3 > S4 > S2 > S1, Elongation (ductility): S1 > S2 > S4 > S3, Impact toughness: S4 > S2 > S1 > S3, and Fatigue limit and fatigue life: S4 > S2 > S3 > S1.

These results emphasize that the optimization of CK45 steel cannot be based solely on maximizing strength. Instead, a balanced combination of hardness, strength, toughness, and fatigue resistance is required to ensure long-term structural integrity and service durability. Based on the comprehensive evaluation of all mechanical and fatigue properties, the quenched–tempered condition (S4) emerges as the optimum thermal processing route for CK45 steel components operating under repeated loading conditions. This treatment provides superior fatigue reliability while maintaining high strength and adequate ductility, making it particularly suitable for shafts, gears, connecting rods, axles, and other engineering components subjected to cyclic stresses and impact loading.

CONCLUSION

This study systematically investigated the influence of thermal processing on the mechanical integrity and fatigue performance of CK45 carbon steel through a comprehensive evaluation of its microstructural evolution, hardness, tensile behavior, impact toughness, and fatigue characteristics. The results demonstrated that thermal treatment significantly altered the microstructure of CK45 steel, leading to substantial changes in its overall performance. The as-received specimen exhibited a coarse ferrite–pearlite structure associated with moderate hardness, strength, and fatigue resistance but excellent ductility. Normalization refined the ferrite–pearlite microstructure, resulting in improvements in hardness, tensile strength, impact toughness, and fatigue performance while maintaining acceptable elongation. Quenching transformed the microstructure into predominantly martensitic phases, producing the highest hardness (55.4 ± 0.9 HRC), yield strength (1015 ± 18 MPa), and ultimate tensile strength (1185 ± 20 MPa). However, these improvements were accompanied by a considerable reduction in elongation (8.2 ± 0.4%) and impact toughness (18 ± 2 KJ) due to the brittle nature of martensite and the presence of residual stresses. Subsequent tempering effectively relieved internal stresses and converted the brittle martensitic structure into tempered martensite containing finely dispersed carbides. Consequently, the quenched–tempered condition exhibited the most balanced mechanical response, combining high hardness (44.1 ± 0.8 HRC), elevated tensile strength (985 ± 18 MPa), improved ductility (14.6 ± 0.5%), the highest impact toughness (68 ± 3 KJ), and superior fatigue performance, characterized by a fatigue limit of 395 ± 13 MPa and a fatigue life of 9.4×10^5 cycles at 500 MPa. The findings confirm that thermal processing is an effective approach for tailoring the performance of CK45 steel. Among the investigated conditions, the quenched–tempered treatment emerged as the optimum route, offering the best compromise between strength,

*Corresponding author
Mohammed RASHEED,
Production Engineering & Metallurgy College, University of Technology- Iraq, Baghdad 10066, Iraq
e-mail: rasheed.mohammed40@yahoo.com

toughness, and fatigue reliability for engineering components subjected to cyclic and impact loading conditions

REFERENCES

[1] B. Chandra Kandpal, H. Kumar, and A. Kumar, "Effect of heat treatment on properties and microstructure of steels," *Materials Today: Proceedings*, vol. 44, pp. 199–205, 2021. https://doi.org/10.1016/j.matpr.2020.09.586
[2] M. Soleimani, H. Mirzadeh, and C. Dehghanian, "Effects of spheroidization heat treatment and intercritical annealing on mechanical properties and corrosion resistance of medium carbon dual phase steel," *Materials Chemistry and Physics*, vol. 257, p. 123721, 2021. https://doi.org/10.1016/j.matchemphys.2020.123721
[3] M. Ravindran, M. Aswatha, N. Santhosh, G. Ravichandran, and M. Madhusudhan, "Effect of heat treatment on fatigue characteristics of EN8 steel," *IOP Conference Series: Materials Science and Engineering*, vol. 1013, p. 012009, 2021. https://doi.org/10.1088/1757-899X/1013/1/012009
[4] K. Kishore, S. Chhangani, M. J. N. V. Prasad, and K. Bhanumurthy, "Microstructure evolution and hardness of hot-dip aluminized coating on pure iron and EUROFER97 steel: Effect of substrate chemistry and heat treatment," *Surface and Coatings Technology*, vol. 409, p. 126783, 2021. https://doi.org/10.1016/j.surfcoat.2021.126783
[5] J. S. Siqueira, M. R. Abreu Alves, T. Marcial Luiz, and R. A. Renzetti, "Effect of heat treatment on the chromium-depleted zones of a high carbon martensitic stainless steel," *Materials and Corrosion*, vol. 72, no. 11, pp. 1752–1761, 2021. https://doi.org/10.1002/maco.202112618
[6] J. N. Ndumia, J. Zhu, B. V. Gbenontin, M. Kang, X. Liu, and S. M. Nyambura, "Effect of heat treatment on the microstructure and corrosion behavior of arc-sprayed FeCrAl/Al coating," *Journal of Materials Engineering and Performance*, vol. 31, pp. 4693–4705, 2022. https://doi.org/10.1007/s11665-021-06473-2
[7] R. Zellagui et al., "Effect of heat treatments on the microstructure, mechanical, wear and corrosion resistance of casted Hadfield steel," *International Journal of Metalcasting*, vol. 16, no. 4, pp. 2050–2064, 2022. https://doi.org/10.1007/s40962-021-00733-z
[8] S. Murmu, S. K. Chaudhary, and A. K. Rajak, "Effect of heat treatment on mechanical properties of medium carbon steel welds," *Materials Today: Proceedings*, vol. 56, pp. 964–970, 2022. https://doi.org/10.1016/j.matpr.2021.11.404
[9] H. Dong, P. F. Guo, Y. Han, R. X. Bai, Z. C. Yang, and S. Q. Zhang, "Enhanced corrosion resistance of high-speed laser-cladded Ni/316L alloy coating by heat treatment," *Journal of Materials Research and Technology*, vol. 24, pp. 952–962, 2023. https://doi.org/10.1016/j.jmrt.2023.03.102
[10] S. Uppada, R. Koona, V. B. Chintada, and R. Koutavarapu, "Influence of heat treatment on crystal structure, microhardness and corrosion resistance of bilayer electroless Ni–P–SiC/Ni–P–Al_2O_3 coatings," *Silicon*, vol. 15, no. 2, pp. 793–803, 2023. https://doi.org/10.1007/s12633-022-01836-6
[11] D. T. Yu, C. L. Wu, S. Zhang, C. H. Zhang, H. T. Chen, and X. P. Tao, "Effects of heat treatment on the nano-indentation, corrosion and cavitation erosion behavior of 17-4PH stainless steel," *Journal of Materials Research and Technology*, vol. 22, pp. 1969–1981, 2023. https://doi.org/10.1016/j.jmrt.2022.12.083
[12] B. M. Edun, O. O. Ajayi, P. O. Babalola, and O. O. Joseph, "The impact of selected bio-based carburising agents on mechanical and tribocorrosion behaviour of medium carbon steel," *Journal of Bio- and Tribo-Corrosion*, vol. 10, no. 4, 2024. https://doi.org/10.1007/s40735-024-00873-1
[13] A. Kumar, P. Singh, and R. Kumar, "Effect of quenching and tempering on the microstructure and tensile properties of medium-carbon steels," *Materials Today: Proceedings*, vol. 72, pp. 1462–1468, 2024. https://doi.org/10.1016/j.matpr.2023.08.214
[14] Y. Li, X. Wang, J. Zhang, and Z. Liu, "Microstructure evolution and fatigue behavior of heat-treated carbon steels under cyclic loading," *Engineering Failure Analysis*, vol. 156, p. 107725, 2024. https://doi.org/10.1016/j.engfailanal.2024.107725

*Corresponding author
Mohammed RASHEED,
Production Engineering & Metallurgy College, University of Technology- Iraq, Baghdad 10066, Iraq
e-mail: rasheed.mohammed40@yahoo.com

[15] B. Chatterjee, S. Das, and A. Mukhopadhyay, "Correlation between microstructure and fatigue performance of quenched and tempered steels," *Materials Characterization*, vol. 208, p. 113522, 2024. https://doi.org/10.1016/j.matchar.2024.113522
[16] I. Aichouch, A. El Magri, and B. Hammouti, "Influence of laser power and scan speed on porosity, microhardness, and corrosion resistance in additively manufactured H13 tool steel," *Progress in Additive Manufacturing*, 2025. https://doi.org/10.1007/s40964-025-00761-7
[17] D. Luca et al., "Structure and mechanical properties of tubular steel components subjected to severe processing," *Crystals*, vol. 15, no. 10, p. 836, 2025. https://doi.org/10.3390/cryst15100836
[18] S. E. Eftekhari Shahri et al., "Recycling CK45 steel chips via spark plasma sintering: Enhanced mechanical and corrosion properties," *Proceedings of the Institution of Mechanical Engineers, Part J: Journal of Engineering Tribology*, 2025. https://doi.org/10.1177/09544089251374752
[19] E. Miftah, "The impact of heat treatment on hardness and corrosion resistance of medium carbon steel," *International Journal of Electrical Engineering and Sustainability*, vol. 3, no. 2, pp. 47–57, 2025. https://doi.org/10.65998/ijees.v3i2.121
[20] D. Zhang, Y. Chen, H. Wu, and L. Zhao, "Recent advances in fatigue behavior and fracture mechanisms of heat-treated medium-carbon steels," *Metals*, vol. 15, no. 2, p. 184, 2025. https://doi.org/10.3390/met15020184
[21] I. Alshalal, H. M. I. Al-Zuhairi, A. A. Abtan, M. Rasheed, M. K. Asmail. J. Mech. Behav. Mater. 32 (2023) 1. https://doi.org/10.1515/jmbm-2022-0280
[22] A. Zubaidi, L.M. Asaad, I. Alshalal, M. Rasheed, J. Mech. Behav. Mater. 32 (2023) 1. https://doi.org/10.1515/jmbm-2022-0302
[23] H. M. I. Al-Zuhairi, I. Alshalal, H. H. Abbood, and M. Al Nuaimi, "Synergistic effects of SiC nanoparticles reinforcement on mechanical performance and microstructural features of Al2024 alloy," *Experimental and Theoretical NANOTECHNOLOGY*, vol. 10, no. S.2, pp. 855–868, May 2026. https://doi.org/10.56053/10.s.855
[24] H. M. I. Al-Zuhairi, I. Alshalal, H. H. Abbood, and M. Al Nuaimi, "Strengthening of aluminum piston alloy through Al2O3 nanoparticles incorporation," *Experimental and Theoretical NANOTECHNOLOGY*, vol. 10, no. S.2, pp. 1093–1107, May 2026. https://doi.org/10.56053/10.s.1093
[25] H. M. I. Al-Zuhairi, I. Alshalal, H. H. Abbood, and M. Al Nuaimi, "Synergistic effects of SiC nanoparticles reinforcement on mechanical performance and microstructural features of Al2024 alloy," *Experimental and Theoretical NANOTECHNOLOGY*, vol. 10, no. S.2, pp. 855–868, May 2026. https://doi.org/10.56053/10.s.855.

*Corresponding author
Mohammed RASHEED,
Production Engineering & Metallurgy College, University of Technology- Iraq, Baghdad 10066, Iraq
e-mail: rasheed.mohammed40@yahoo.com